


Computer-aided Evaluation of Anti-SARS-CoV-2 (3-chymotrypsin-like Protease and Transmembrane Protease Serine 2 Inhibitors) Activity of Cepharanthine: An *In silico* Approach

Divya Jain ¹, Rajib Hossain ², Rasel Ahmed Khan ³, Dipta Dey ⁴, Tanzila Rahman Toma ⁵, Mohammad Torequl Islam ², Pracheta Janmeda ¹, Khalid Rehman Hakeem ^{6,*} 

¹ Department of Bioscience and Biotechnology, Banasthali Vidyapith, Rajasthan-304022, India; divyajain31011996@gmail.com; pracheta@banasthali.in (P.J.);

² Department of Pharmacy, Life Science Faculty, Bangabandhu Sheikh Mujibur Rahman Science and Technology University, Gopalganj-8100, Bangladesh; rajibhossainrh021@gmail.com (R.H.); mti031124@gmail.com (M.T.I.);

³ Pharmacy Discipline, Life Science School, Khulna University, Khulna, Bangladesh; raselahmed358@gmail.com (R.A.K.);

⁴ Department of Biochemistry and Molecular Biology, Life Science Faculty, Bangabandhu Sheikh Mujibur Rahman Science and Technology University, Gopalganj-8100, Bangladesh; diptadey727@gmail.com (D.D.);

⁵ Institute of Social Welfare and Research, University of Dhaka, Dhaka, Bangladesh; tanzilarahman95t@gmail.com (T.R.T.);

⁶ Department of Biological Sciences, Faculty of Science, King Abdulaziz University, Jeddah, Saudi Arabia; kur.hakeem@gmail.com (K.R.H.);

* Correspondence: kur.hakeem@gmail.com;

Scopus Author ID 36993011800

Received: 28.02.2021; Revised: 4.04.2021; Accepted: 8.04.2021; Published: 26.04.2021

Abstract: 3-chymotrypsin-like protease (3CL^{PRO}) is found in severe acute respiratory syndrome coronavirus (SARS CoV)-2, and transmembrane protease serine 2 (TMPRSS-2) in humans, both of them have a role in viral attachment and proliferation. 3CL^{PRO} and TMPRSS-2 are the most vital target for the discovery of an anti-corona virus. One efficient approach used to screen potential active compounds against specific target proteins, such as 3CL^{PRO} and TMPRSS-2, is molecular docking. Cepharanthine (CEP) exhibits antiviral activity in SARS-CoV at 9.5 µg/mL IC₅₀ level. This study aims to perform an *in silico* study on CEP against non-structural SARS-CoV-2 3CL^{PRO} and host transmembrane protease serine 2 protein. Molecular docking studies were carried out using compounds against 3CL^{PRO} and TMPRSS-2 proteins through Swiss model, Uniport, PROCHECK, Swiss PDB viewer, PyMol, and PyRx computerized software. CEP displayed strong binding interactions -8.5 and -7.4 Kcal/mol with the 3CL^{PRO}, and TMPRSS-2 proteins. In all cases, CEP showed better binding affinities than FDA-approved anti-corona virus drug (Camostat mesylate, CAM) is currently underused in COVID-19. CEP may be one of the potentials leads to fighting against SARS-CoV-2. Further *in vivo* studies should be required to support the findings of this study.

Keywords: Cepharanthine; COVID-19; 3CL^{PRO}; molecular docking; pkCSM, Swiss-ADME; TMPRSS2.

© 2021 by the authors. This article is an open-access article distributed under the terms and conditions of the Creative Commons Attribution (CC BY) license (<https://creativecommons.org/licenses/by/4.0/>).

1. Introduction

Novel coronavirus (Coronaviridae family) [1, 2] is a pathogenic microorganism that primarily targets the human respiratory tract, causing fever, fatigue, dry cough, muscle aches,

shortness of breath, loss of taste or smell, headache, and sometimes pneumonia [3-5]. The severe acute respiratory syndrome coronavirus 2 (SARS CoV-2) is a single-stranded RNA virus along with 29,903 nucleotides base-pair genome sequence [6-9].

In 2019, coronavirus became a pandemic worldwide [10]. Two categories of proteins are identified in SARS CoV-2, includes structural proteins and non-structural proteins. In structural proteins involves Spike (S), Nucleocapsid (N), Matrix (M), and Envelope (E), and the non-structural proteins are 3- chymotrypsin-*like* protease (3CL^{PRO}), Papain-*like* protease (PL^{PRO}), and RNA-dependent RNA polymerase (RdRp) [7]. The CoV-2 polyprotein encodes two protease- 3-chymotrypsin-*like* protease (M^{PRO} or 3CL^{PRO}) and papain-*like* protease (PL^{PRO}) [11], which are responsible for transcription and replication of the proteins in the viral genome [12].

It catalytically cleaved the conserved sites in polyprotein 1ab (PP1ab) and 1a (PP1a) [13]. The structure and catalytic mechanism of 3CL^{PRO} consider it as a selective target for drug development for coronavirus. Coronavirus can synthesis a precursor protein, essential for virus fusion to the host cell membrane (human cell), cleavage by TMPRSS2 (a host cell proteases) [14, 15]. Whereas the TMPRSS2 facilitates hCoVs, including SARS-CoV-2 infections, via two independent mechanisms: (i) proteolytic cleavage of hACE2R, which promotes viral uptake, and (ii) cleavage of CoV S proteins which activates the glycoprotein for host cell entry [16]. It has also been suggested that the intestine is one of the potential sites of SARS-CoV-2 replication. Besides, TMPRSS2 and TMPRSS4 were seen to facilitate SARS-CoV-2 spike fusogenic activity, thereby promoted virtual entrance into the host [17]. Hence, protease inhibitors should be the drug target for treating or preventing viral infections. On the other hand, serine protease inhibitors can suppress viral proliferation [18, 19].

Cepharanthine (C₃₇H₃₈N₂O₆, CEP) is a biscoclaurine alkaloid containing a methylenedioxy group [20, 21], isolated from *Stephania* [22]. Cepharanthine is a potential lead with significant antiviral activity against viruses, including HIV, HTLV, HBV, SARS-CoV. In SARS-CoV, Cepharanthine inhibits protease at 9.5 µg/ML [23]. Besides this, it has many important biological activities, such as antioxidant [24], anti-tumor [25], anti-inflammatory, antineoplastic [22], anticancer, anti-sickness [23], antiparasitic [26] activities.

In exploring novel therapies for COVID-19, researchers use computational approaches to aid in discovering potential candidates [27-29]. Two essential strategies should be followed by the researcher for the development of new coronavirus drugs. Firstly, inhibitors should have the ability to block virus entry into the host cells, and secondly, compounds that attenuate viral transcription and cell replication. One efficient approach used to screen potential active compounds against specific target proteins, such as 3CL^{PRO} and TMPRSS2 are molecular docking simulation. Therefore, these are important targets for the design of potential anti-CoV inhibitors.

2. Materials and Methods

2.1. Computational homology modeling and macromolecule preparation.

For modeling, the sequence of 3CL^{PRO}, and TMPRSS2 were poised from UniProt [30] followed by BLAST analysis using the NCBI BLAST program [31]. Computational homology modeling was carried out by Swissmodel [32]. Then, to validate the homology model acquired from the Swiss model, PROCHECK [33] online-based software was employed. After that, with these protein model docking was performed for binding interactions. A swiss-PDB Viewer

software package (version 4.1.0) was utilized for energy minimization of structures, and before docking, PyMOL (version 1.7.4.5) was performed for removing all the heteroatoms and water molecules from proteins [34].

2.2. Ligand preparation.

The ligands, Cepharanthine (CEP) (PubChem ID: 10206) and FDA-approved antiviral drugs Camostat mesylate (CAM) (PubChem ID: 5284360) (Figure 1) were downloaded from the PubChem in the 'sdf' file format. Using Chem3D Pro12.0 program packages [35], all internal energies of the ligands molecule were optimized. The Nation Centre maintains the system for Biotechnology Information (NCBI), a component of the National Library of Medicine.

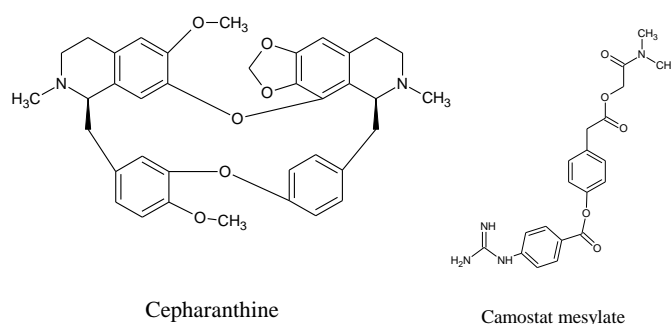


Figure 1. The chemical structure of Cepharanthine and Camostat mesylate (drawn by chem sketch v12.1.0.31258).

2.3. Docking analysis and binding site.

In drug discovery and development study, molecular docking is a system that is used for predicting the drug candidate's pharmacodynamics profile by scoring and orienting them to the receptor binding sites by PyRx-virtual screening tool [36]. The docking result determines the measure of ligand interaction to the active site of the targeted protein. The actives sites are the coordinates of the ligand in the original target protein grids [37] through PyMol and Drug Discovery Studio version 4.5 is used for scrutinizing these active binding sites of the target protein [38].

2.4. ADMET prediction.

Various pharmacokinetic properties (absorption, distribution, metabolism, excretion, and toxicity parameters) of CEP were predicted using pkCSM and Swiss ADME online-based computer software [39, 40]. The ADMET parameters of CEP were mainly analyzed. The website was logged on and the SMILES of CEP data from PubChem were searched and submitted to the website, ADMET mode in pkCSM, and ADME mode in Swiss-ADME was selected.

2.5. Target prediction.

For discovering and developing a drug, it has been important to find the phenotypical side effects or potential cross-reactivity for bioactive compounds. For finding side effects or cross-reactivity, Molecular Target studies are essential [41, 42]. Swiss Target Prediction is an online-based website. For searching the targets, the canonical SMILES of CEP were entered into the search bar and were analyzed.

3. Results and Discussion

3.1. Homology modeling.

The SARS CoV-2 3CL^{PRO} (Uniprot accession ID: P0DTD1), and TMPRSS2 (Uniprot accession ID: O15393) amino acid were collected from, were subjected to NCBI Blast Program for selection of the closest homologous template Homology model of 3CL^{PRO}, and TMPRSS2 was generated by Swiss model (Figure 2). Optimization of 3CL^{PRO} and TMPRSS2 was achieved using the Swiss-PDB Viewer software package (version 4.1.0) before docking. At the same time, validation of these 3CL^{PRO}, and TMPRSS2 homology models were acquired through the use of the Ramachandran plot performed by PROCHECK and illustrated in Figure 3.

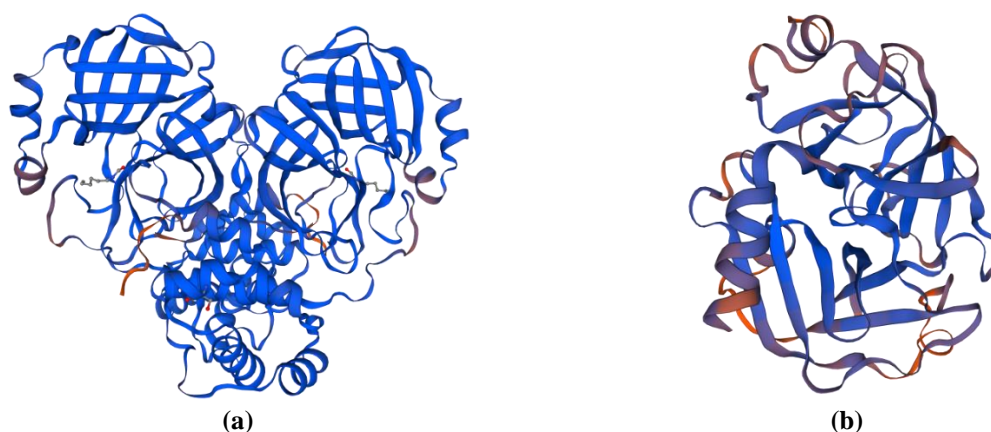


Figure 2. Three-dimensional structures of the (a), SARS-CoV-2 3CLPRO, and (b). TMPRSS2 is predicted by the Swiss model.

3.2. Amino acid interaction of Cepharanthine and Camostat mesylate with SARS-CoV-2 3CL^{PRO}, and human TMPRSS-2.

Today, anti-corona virus drugs are the crying need for treating COVID-19. So many people have died for SARS-CoV-2 worldwide. Several antiviral drugs like Ritonavir, Lopinavir, Indinavir, and Remdesivir, and Camostat mesylate are used for the trial to possess a cure for showing the anti-Coronavirus effect [43]. But in some emergency cases, hydroxychloroquine and azithromycin are shown potent effects [44-46], but the complex showed adverse side effects. An equally or more potent natural compound should be found out by researchers that are safe and have fewer side effects. Cepharanthine is an excellent candidate for anti-Coronavirus agents because of its biological properties. It can be isolated from *Stephania* [22].

3CL^{PRO} can provide a transcript and replicate the viral genome [12], whereas the TMPRSS2 facilitates hCoVs, including SARS-CoV-2 infections, via two independent mechanisms. First, it promotes viral uptake through proteolytic cleavage of hACE2R, and secondly, cleavage of CoV-2 Spike proteins [16].

The reference inhibitor's interactions and selected biscoclaurine alkaloid with 3-chymotrypsin-like protease (3CL^{PRO}) of coronaviruses and human transmembrane protease serine-2 (TMPRSS-2) are represented in Table 1. The ligand molecule mostly exhibited interaction with target proteins amino acid residues through hydrophobic interactions. Some H-bonding was also seen, but it was Carbon-Hydrogen interaction.

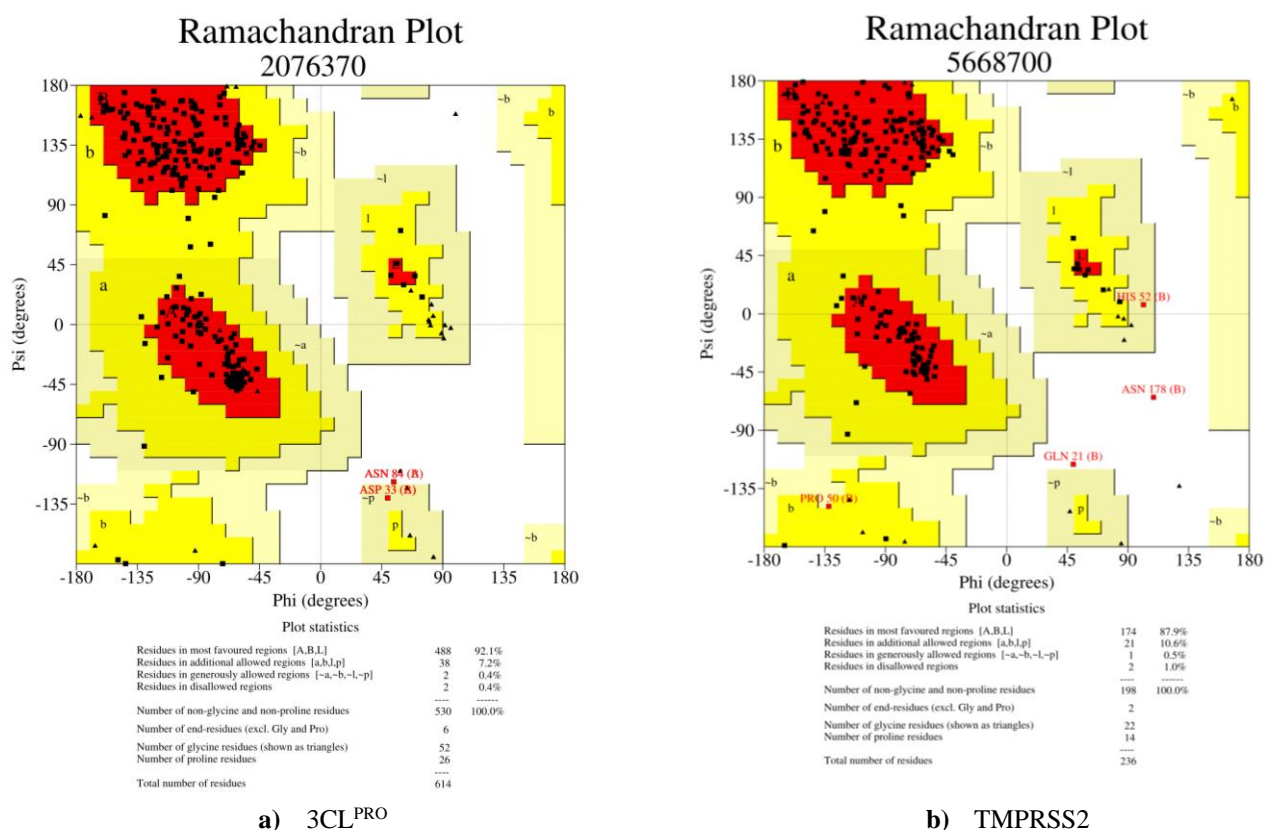


Figure 3. The optimized model of the SARS CoV-2 (a) 3CL^{PRO} and (b) human TMPrSS-2 using PROCHECK.

The ligand-protein binding interactions analysis showed CEP exhibited good binding affinities -8.5 and -7.4 kcal/mol with 3CL^{PRO} and TMPrSS-2, respectively. It showed binding interactions with 3CL^{PRO} through four bonds like carbon-hydrogen, alkyl, and pi-alkyl, with Ile249 and Pro293, and Pi-anion with Asp245 amino acid residues. Besides, with TMPrSS-2, CEP interacts through Lys107, Trp198, Cys110, Ile197, Lys107, Pro13, Trp14 amino acids in the receptor pocket. Two carbon-hydrogen bonds with Lys107, Trp198 amino acid residues and π -S, π - π , π -alkyl bonds with Cys110, Trp14, Ile197, Lys107, Pro13, respectively.

In a computational molecular docking study, CEP is successfully docked against 3CL^{PRO}, and TMPrSS2 inhibitor regions with a docking score of -8.5 and -7.4 Kcal/mol, respectively. Furthermore, it exerts good binding affinities compared with lopinavir, oseltamivir, and ritonavir, whose binding affinities are -4.1 Kcal/mol, -4.65 Kcal/mol, and -5.11 Kcal/mol [47]. Moreover, some plant-derived flavonoid and polyphenolic compounds such as kaempferol, quercetin, demethoxycurcumin, curcumin, catechin, epicatechingallate, gingerol, and gingerol can inhibit the main protease of SARS-CoV-2 in silico study whose binding affinities are -9.41 Kcal/mol, -8.58 Kcal/mol, -8.17 Kcal/mol, -7.31 Kcal/mol, -7.05 Kcal/mol, -7.24 Kcal/mol, -6.67 Kcal/mol and -5.40 Kcal/mol respectively.

Table 1. Docking results of cepharanthine (CEP) and reference compound, camostat mesylate (CAM) with the SARS-CoV2 (3CL^{PRO}), and human TMPrSS2 proteins therapeutic target.

Drug-Protein complex	Docking score (kcal/mol)	No of H-Bond	Amino acid residues
CEP-3CL ^{PRO}	-8.5	1	Ile249 (H), Pro293, Asp245.
CEP-TMPrSS2	-7.4	2	Lys107 (H), Trp198 (H), Cys110, Ile197, Lys107, Pro13, Trp14.
CAM-3CL ^{PRO}	-7.4	4	Asp153 (H), Asn151 (H), Ile249(H), Ser158(H), Ile106, Phe294.
CAM-TMPrSS2	-7.4	2	Lys68 (H), Asp67, Ile135, Leu132, Phe66, Phe118, Pro53.

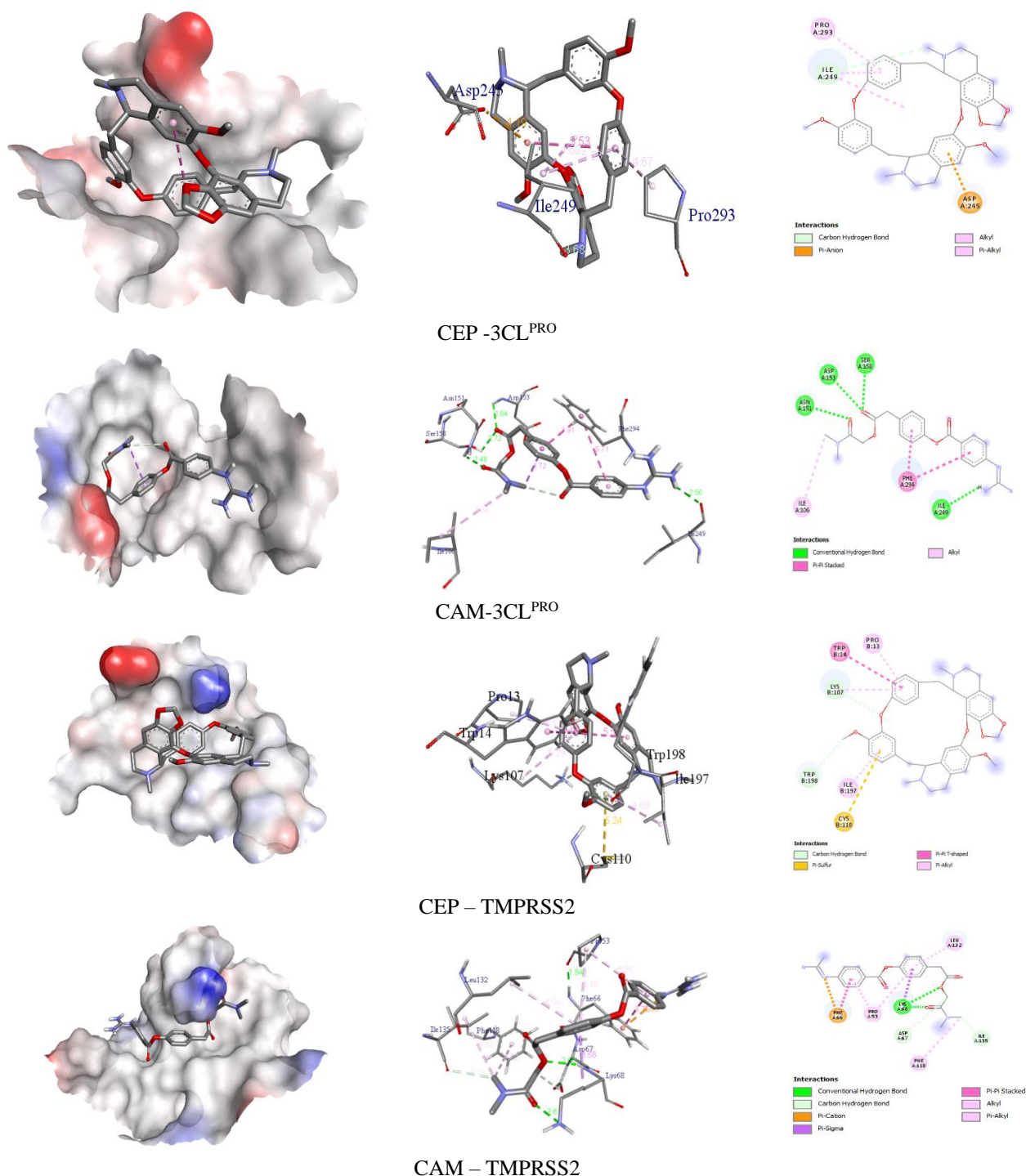


Figure 4. Interactions of cepharanthine (CEP) and camostat mesylate (CAM) with the SARS-CoV-2 and host proteins (TMPRSS-2).

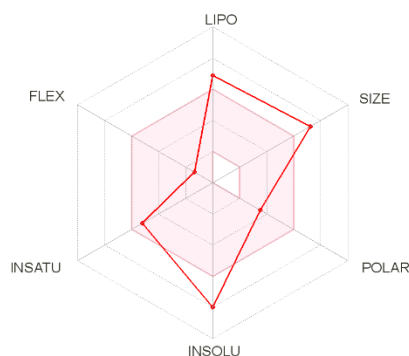
In this study, the docking score of cepharanthine is higher. Even the proposed inhibitor of SARS CoV-2, such as camostat mesylate, has a docking score of -7.4 Kcal/mol, which claimed that CEP has better properties than camostatmesylate and other combinations therapy. A study suggested that CEP at 9.5 $\mu\text{g/mL}$ IC₅₀ concentration inhibits SARS CoV protease [48].

Camostat mesylate (CAM) is a synthetic compound used as a serine protease inhibitor [49, 50], which was first mentioned in the literature in 1981, as askin tumors inhibitors in mice models. Furthermore, it can inhibit cholecystokinin, pro-inflammatory cytokines, and serine proteases and treat COVID-19 [51-53].

On the other hand, the standard drug (Camostat mesylate, CAM) showed good binding interaction (-7.4 kcal/mol) with 3CL^{PRO} and TMPRSS2 (Table 1). The hydroxyl group of Asp153, Asn151, Ile249, Ser158 at a distance of 2.48, 2.84, 2.56, and 2.72 Å, respectively, while the π - π interaction of Phe294 and alkyl interaction of Ile106 exhibiting hydrophobic interaction. Similarly, the hydroxyl group of CAM also mediates two hydrogen bond interactions with Lys68 with a distance of 2.60 and 2.61 Å with TPMRSS-2 receptor amino acids. Additionally, multiple hydrophobic interactions were observed with Asp67, Ile135, Leu132, Phe66, Phe118, and Pro53. The 2D and 3D structures of non-bond interactions of CEP and CAM with the target proteins have been illustrated in Figure 4.

3.3. Physiochemical, pharmacokinetics, and toxicological properties assessment of CEP.

From online-based software data, it has been found that CEP has a molecular weight of 606.71 g/mol with 45 heavy atoms and 0.35 Fraction Csp3 (Figure 5). It has 2 rotatable bonds, 8 H-bond acceptors but no H-bond donors. Molar refractivity is 179.15, and TPSA is 61.86 Å². The molecule's lipophilicity in terms of Log $P_{o/w}$ (iLOGP), Log $P_{o/w}$ (XLOGP3), Log $P_{o/w}$ (WLOGP), Log $P_{o/w}$ (MLOGP), Log $P_{o/w}$ (SILICOS-IT) was found 5.06, 6.54, 5.46, 3.96 and 5.71 respectively. It's a poorly soluble material with Log S (ESOL) value of -7.98 and solubility value of 6.29e-06 mg/ml; 1.04e-08 mol/l.



The color space is a suitable physiochemical space for oral bioavailability.

LIPO Lipophilicity: $-0.7 < \text{XLOGP3} < 5.0$.

SIZE: $150\text{g/mol} < \text{MW} < 500\text{g/mol}$.

POLAR (Polarity): $20\text{\AA}^2 < \text{TPSA} < 130\text{\AA}^2$.

INSOLU (insolubility): $0 < \text{Log } S \text{ (ESOL)} < 6$.

INSATU (insaturation): $0.25 < \text{Fraction Csp3} < 1$.

FLEX (Flexibility): $0 < \text{Num. rotatable bonds} < 9$

Figure 5. Summary of physiochemical, pharmacokinetics, and toxicological properties of Cepharanthine.

In the computational docking study, CEP displayed good interaction with TMPRSS2 and inhibit serine protease. Some studies suggested that CEP is an antioxidant and anti-inflammatory agent. It can attenuate oxidative stress and inflammation in several testing systems [22, 24]. Additionally, CEP is cytotoxic effects on the existing viruses [54, 55]. Therefore, CEP should have cytotoxic effects on the existing SARS CoV-2. When a compound has followed four basic criteria, it should be an ideal anti-COVID-19 drug. CEP can restrict viral entrance by inhibiting cellular attachment. It can attenuate viral replication and cytotoxic effects on the existing viruses. And finally, it can protect the normal host cells from the viral origin oxidative stress and inflammatory responses, and CEP meets all the requirements.

Several studies suggested that small molecules should have <500gm/mol for acceptability, for considering a drug, whereas CEP has a slightly higher molecular weight. A range of H-bond acceptors and H-bond donors with ≤ 10 and ≤ 5 are acceptable. It has also been suggested that the molar refractivity of compounds ranging from 40-130, lipophilicity (LogP) is <5 is accepted.

CEP shows high GI absorption without any BBB permeation, P-gp substrate, and CYP50 inhibitor, whereas Log K_p (skin permeation) is -5.36 cm/s. In terms of drug-likeness CEP complies with Lipinski's rule of five, showing 1 violation (MW>500), which violates 3 parameters of the Ghose rule (MW>480, MR>130, #atoms>70), complies to Veber and Egan rules. CEP has 3 violations of Muegge rule (No; 3 violations: MW>600, XLOGP3>5, #rings>7). The bioavailability score CEP is 0.55. The compound has shown zero PAINS and Brenk alert. It showed 2 violations in the Leadlikeness score (MW>350, XLOGP3>3.5) along with 7.01 synthetic accessibility (Table 2).

Table 2. Predicted Physicochemical, drug-likeness, and ADME properties of the selected compound by Swiss ADME.

Physicochemical Properties	
Molecular weight	606.71 g/mol
Num. heavy atoms	45
Fraction Csp3	0.35
Num. rotatable bonds	2
Num. H-bond acceptors	8
Num. H-bond donors	0
Molar Refractivity	179.15
TPSA	61.86 Å ²
Lipophilicity	
Log $P_{o/w}$ (iLOGP)	5.06
Log $P_{o/w}$ (XLOGP3)	6.54
Log $P_{o/w}$ (WLOGP)	5.46
Log $P_{o/w}$ (MLOGP)	3.96
Log $P_{o/w}$ (SILICOS-IT)	5.71
Water Solubility	
Log S (ESOL)	-7.98
Solubility	6.29e-06 mg/ml ; 1.04e-08 mol/l
Class	Poorly soluble
Pharmacokinetics	
GI absorption	High
BBB permeant	No
P-gp substrate	No
CYP50 inhibitor	No
Log K_p (skin permeation)	-5.36 cm/s
Drug-likeness	
Lipinski	Yes; 1 violation: MW>500
Ghose	No; 3 violations: MW>480, MR>130, #atoms>70
Veber	Yes
Egan	Yes
Muegge	No; 3 violations: MW>600, XLOGP3>5, #rings>7
Bioavailability Score	0.55
Medicinal Chemistry	
PAINS	0 alert
Brenk	0 alert
Leadlikeness	No; 2 violations: MW>350, XLOGP3>3.5
Synthetic accessibility	7.01

Upon toxicity testing, CEP displayed positive AMES toxicity also; the tolerable maximum tolerable dose in humans is 0.232 mg/kg/day. It has shown no hERG I inhibitor activity but shown hERG II inhibitor activity. The LD₅₀ value for oral rat acute toxicity is 2.554, and the LOAEL value is 0.711 while showing no hepatotoxicity and skin sensitization (Table 3).

The drug-likeness evaluates the probability for a molecule to turn an oral drug concerning bioavailability. The Lipinski is the pioneer rule of five [56], and the Ghose, Veber, Egan, and Muegge were performed in case of drug-likeness [57-60]. The Bioavailability Score pursues to compute a compound's probability to have oral bioavailability in rat or measurable Caco-2 permeability [61]. Here, PAINS are the molecules carrying substructures exhibiting optimal response in assays irrespective of the protein target [62-64].

Brenk *et al.*, [62] reported a list of 105 fragments for the structural alert. Our study revealed zero alerts of PAINS and Brenk. Leadlikeness is subjected to chemical modifications that can enhance the size and lipophilicity of the compound, and the leads are requisite to be lesser and small hydrophobicity [65]. Synthetic accessibility (SA), in the selection of suitable virtual molecules, is a chief factor. Medicinal chemists, for a reasonable number of molecules, are the best able to determine SA. The SA Score ranges from 1-10 (very easy-very difficult to synthesize), after normalization [66]. Moreover, it has no hepatotoxicity and skin sensitization.

Table 3. Toxicological properties of Cepharanthine.

Property	Model Name	Predicted Value	Unit
Toxicity	AMES toxicity	Yes	Categorical (Yes/No)
	Max. tolerated dose (human)	0.232	Numeric (log mg/kg/day)
	hERG I inhibitor	No	Categorical (Yes/No)
	hERG II inhibitor	Yes	Categorical (Yes/No)
	Oral Rat Acute Toxicity (LD50)	2.554	Numeric (mol/kg)
	Oral Rat Chronic Toxicity (LOAEL)	0.711	Numeric (log mg/kg bw/day)
	Hepatotoxicity	No	Categorical (Yes/No)
	Skin Sensitisation	No	Categorical (Yes/No)

3.4. Target prediction.

The pie chart is the best way to display several subjects at a time. For target prediction analysis, the top 15 of the results were given as pie-chart are illustrated in figure 6. The pie chart displayed 40 % of family A G protein-coupled receptor, 13.3% of electrochemical transporter, 6.7% of Hydrolase, phosphodiesterase, membrane receptor, and 26.7% of a ligand-gated ion channel. The Target, Common Name, Uniprot ID, ChEMBL-ID, Target Class, Probability, and Known actives in 2D/3D are given in the output table.

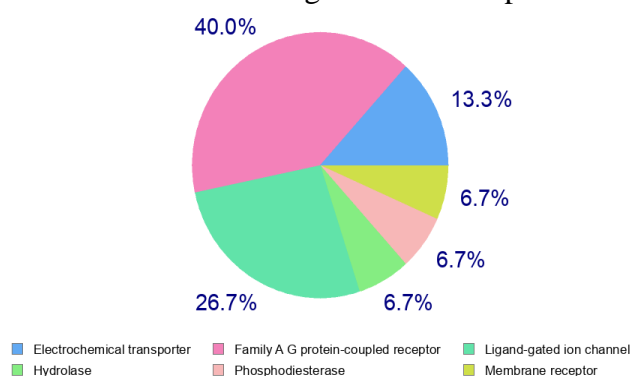


Figure 6. Top-15 of Target Predicted for Cepharanthine.

Furthermore, target prediction data suggested that if cepharanthine showed any adverse pharmacological effect in the testing system, where are the possible binds create with the target by Cepharanthine. It has been predicted that cepharanthine is most probably bound with family-A G protein-coupled receptor, electrochemical transporter, hydrolases, phosphodiesterase, membrane receptor, and ligand-gated ion channel.

From the predicted *in silico*, physiochemical, drug-likeness, and ADME properties, target prediction test data, it has been claimed that CEP is a good candidate for COVID-19 treatment.

4. Conclusions

In summary, the computer-aided analysis was performed for elucidating the activity of cepharanthine, which was found in the *Stephania* plant and could treat SARS-CoV-2 3CL^{PRO} and human TMPRSS-2 targets. Cepharanthine should be possibly used as a lead compound and neutraceuticals involved in COVID-19 treatment. Although further *in vivo* studies are necessary to establish the findings observed in this study, our findings will help further non-clinical, pre-clinical, and clinical studies with this compound. Finally, this study will inspire medicinal scientists to conduct adequate research on this hopeful natural lead compound and its laboratory derivatives.

Funding

This research received no external funding.

Acknowledgments

The authors acknowledge the Bioinformatics Centre, Banasthali Vidyapith supported by DBT and DST for providing computation and networking support through the FIST and CURIE programs at the Department of Bioscience and Biotechnology, Banasthali Vidyapith, Rajasthan, India, and special thanks to the International Centre for Empirical Research and Development (ICERD), and Department of Pharmacy, Life Science Faculty, Bangabandhu Sheikh Mujibur Rahman Science and Technology University, Gopalganj, Bangladesh.

Conflicts of Interest

The authors declare no conflict of interest.

References

1. Boopathi, S.; Poma, A. B.; Kolandaivel, P. Novel 2019 Coronavirus Structure, Mechanism of Action, Antiviral Drug Promises and Rule out against Its Treatment. *J. Biomol. Struct. Dyn.* **2020**, 1–10, <https://doi.org/10.1080/07391102.2020.1758788>.
2. Li, F. Structure, Function, and Evolution of Coronavirus Spike Proteins. *Annu. Rev. Virol.* **2016**, 3, 237–261, <https://doi.org/10.1146/annurev-virology-110615-042301>.
3. Rothan, H.A.; Byrareddy, S.N. The Epidemiology and Pathogenesis of Coronavirus Disease (COVID-19) Outbreak. *J. Autoimmun.* **2020**, 109, <https://doi.org/10.1016/j.jaut.2020.102433>.
4. Ebrahimi, A. Correlation of CoViD-19 Infection and Tumorigenesis. *Letters in Applied NanoBioScience* **2021**, 10, 2578–2587, <https://doi.org/10.33263/LIANBS103.25782587>.
5. Cheke, R.S.; Narkhede, R.R.; Shinde, S.D.; Ambhore, J.P.; Jain, P.G. Repurposing of Anthelmintic Drugs against SARS-CoV-2 (Mpro and RdRp): Novel Disease, Older Therapeutics. *Lett. Appl. NanoBioScience* **2021**, 10, 2331–2338.
6. Masters, P.S. The Molecular Biology of Coronaviruses. *Adv. Virus Res.* **2006**, 66, 193–292, [https://dx.doi.org/10.1016%2FS0065-3527\(06\)66005-3](https://dx.doi.org/10.1016%2FS0065-3527(06)66005-3).
7. Elfiky, A.A.; Mahdy, S.M.; Elshemey, W.M. Quantitative Structure-Activity Relationship and Molecular Docking Revealed a Potency of Anti-Hepatitis C Virus Drugs against Human Corona Viruses. *J. Med. Virol.* **2017**, 89, 1040–1047. <https://doi.org/10.1002/jmv.24736>.
8. Padhy, M. A Review on Medicinal Plants Withania Somnifera and Nyctanthes Arbortristis: Boosting of Immune System During SARS-CoV-2. *Lett. Appl. NanoBioScience* **2020**, 9, 1538–1546, <https://doi.org/10.33263/LIANBS94.15381546>.

9. Krishnakumar, S.; Aabha Benjamin, G. P. W. Outbreak, Prevalence and Mortality of Severe Acute Respiratory Syndrome (SARS-CoV-2) Infections in Kerala- A Perspective Study. *Lett. Appl. NanoBioScience* **2021**, *10*, 2016–2023, <https://doi.org/10.33263/LIANBS101.20162023>.
10. Francés-Monerris, A.; Hognon, C.; Miclot, T.; García-Iriepa, C.; Iriepa, I.; Terenzi, A.; Grandemange, S.; Barone, G.; Marazzi, M.; Monari, A. Molecular Basis of SARS-CoV-2 Infection and Rational Design of Potential Antiviral Agents: Modeling and Simulation Approaches. *J. Proteome Res* **2020**, *19*, 4291–4315, <https://dx.doi.org/10.1021/acs.jproteome.0c00779>
11. Hilgenfeld, R. From SARS to MERS: Crystallographic Studies on Coronaviral Proteases Enable Antiviral Drug Design. *FEBS J* **2014**, *281*, 4085–4096, <https://doi.org/10.1111/febs.12936>.
12. Gyebi, G.A.; Ogunro, O.B.; Adegunloye, A.P.; Ogunyemi, O.M.; Afolabi, S.O. Potential Inhibitors of Coronavirus 3-Chymotrypsin-like Protease (3CLpro): An in Silico Screening of Alkaloids and Terpenoids from African Medicinal Plants. *J. Biomol. Struct. Dyn* **2020**, 1–13, <https://doi.org/10.1080/07391102.2020.1764868>.
13. Anand, K.; Ziebuhr, J.; Wadhwani, P.; Mesters, J.R.; Hilgenfeld, R. Coronavirus Main Proteinase (3CLpro) Structure: Basis for Design of Anti-SARS Drugs. *Science* **2003**, *300*, 1763–1767, <https://doi.org/10.1126/science.1085658>.
14. Böttcher-Friebertshäuser, E.; Freuer, C.; Sielaff, F.; Schmidt, S.; Eickmann, M.; Uhlenndorff, J.; Steinmetzer, T.; Klenk, H.-D.; Garten, W. Cleavage of Influenza Virus Hemagglutinin by Airway Proteases TMPRSS2 and HAT Differs in Subcellular Localization and Susceptibility to Protease Inhibitors. *J. Virol* **2010**, *84*, 5605–5614, <https://doi.org/10.1128/jvi.00140-10>.
15. Yamaya, M.; Shimotai, Y.; Hatachi, Y.; Lusamba Kalonji, N.; Tando, Y.; Kitajima, Y.; Matsuo, K.; Kubo, H.; Nagatomi, R.; Hongo, S.; Homma, M.; Nishimura, H. The Serine Protease Inhibitor Camostat Inhibits Influenza Virus Replication and Cytokine Production in Primary Cultures of Human Tracheal Epithelial Cells. *Pulm. Pharmacol. Ther* **2015**, *33*, 66–74, <https://doi.org/10.1016/j.pupt.2015.07.001>.
16. Shulla, A.; Heald-Sargent, T.; Subramanya, G.; Zhao, J.; Perlman, S.; Gallagher, T. A Transmembrane Serine Protease Is Linked to the Severe Acute Respiratory Syndrome Coronavirus Receptor and Activates Virus Entry. *J. Virol* **2011**, *85*, 873–882, <https://doi.org/10.1128/JVI.02062-10>.
17. Zang, R.; Gomez Castro, M.F.; McCune, B.T.; Zeng, Q.; Rothlauf, P.W.; Sonnek, N.M.; Liu, Z.; Brulois, K.F.; Wang, X.; Greenberg, H.B.; Diamond, M.S.; Ciorba, M.A.; Whelan, S.P.J.; Ding, S. TMPRSS2 and TMPRSS4 Promote SARS-CoV-2 Infection of Human Small Intestinal Enterocytes. *Sci. Immunol* **2020**, *5*, <https://doi.org/10.1126/sciimmunol.abc3582>.
18. Böttcher, E.; Freuer, C.; Steinmetzer, T.; Klenk, H.-D.; Garten, W. MDCK Cells That Express Proteases TMPRSS2 and HAT Provide a Cell System to Propagate Influenza Viruses in the Absence of Trypsin and to Study Cleavage of HA and Its Inhibition. *Vaccine* **2009**, *27*, 6324–6329, <https://doi.org/10.1016/j.vaccine.2009.03.029>.
19. Böttcher-Friebertshäuser, E.; Stein, D. A.; Klenk, H.-D.; Garten, W. Inhibition of Influenza Virus Infection in Human Airway Cell Cultures by an Antisense Peptide-Conjugated Morpholino Oligomer Targeting the Hemagglutinin-Activating Protease TMPRSS2. *J. Virol* **2011**, *85*, 1554–1562.
20. Rogosnitzky, M.; Danks, R. Therapeutic Potential of the Biscoclaurine Alkaloid, Cepharanthine, for a Range of Clinical Conditions. *Pharmacol. Rep* **2011**, *63*, 337–347, [https://doi.org/10.1016/S1734-1140\(11\)70500-X](https://doi.org/10.1016/S1734-1140(11)70500-X).
21. Rogosnitzky, M.; Okediji, P.; Koman, I. Cepharanthine: A Review of the Antiviral Potential of a Japanese-Approved Alopecia Drug in COVID-19. *Pharmacol. Rep* **2020**, *72*, 1509–1516, <https://doi.org/10.1007/s43440-020-00132-z>.
22. Huang, H.; Hu, G.; Wang, C.; Xu, H.; Chen, X.; Qian, A. Cepharanthine, an Alkaloid from *Stephania* *Cepharantha* Hayata, Inhibits the Inflammatory Response in the RAW264. 7 Cell and Mouse Models. *Inflammation* **2014**, *37*, 235–246, <https://doi.org/10.1007/s10753-013-9734-8>.
23. Jeon, S.; Ko, M.; Lee, J.; Choi, I.; Byun, S. Y.; Park, S.; Shum, D.; Kim, S. Identification of Antiviral Drug Candidates against SARS-CoV-2 from FDA-Approved Drugs. *Antimicrob. Agents Chemother* **2020**, *64*, <https://doi.org/10.1128/AAC.00819-20>.
24. Gülçin, I.; Elias, R.; Gepdiremen, A.; Chea, A.; Topal, F. Antioxidant Activity of Bisbenzylisoquinoline Alkaloids from *Stephania* *Rotunda*: Cepharanthine and Fangchinoline. *J. Enzyme Inhib. Med. Chem* **2010**, *25*, 44–53, <https://doi.org/10.3109/14756360902932792>.
25. Seubwai, W.; Vaeteewoottacharn, K.; Hiyoshi, M.; Suzu, S.; Puapairoj, A.; Wongkham, C.; Okada, S.; Wongkham, S. Cepharanthine Exerts Antitumor Activity on Cholangiocarcinoma by Inhibiting NF-κB. *Cancer science* **2010**, *101*, 1590–1595, <https://doi.org/10.1111/j.1349-7006.2010.01572.x>.
26. Desgrouas, C.; Chapus, C.; Desplans, J.; Travaille, C.; Pascual, A.; Baghdikian, B.; Ollivier, E.; Parzy, D.; Taudon, N. In Vitro Antiplasmodial Activity of Cepharanthine. *Malar. J* **2014**, *13*, <https://doi.org/10.1186/1475-2875-13-327>.
27. Ciliberto, G.; Cardone, L. Boosting the Arsenal against COVID-19 through Computational Drug Repurposing. *Drug Discov. Today* **2020**, *25*, 946–948, <https://doi.org/10.1016/j.drudis.2020.04.005>.

28. Ruan, Z.; Liu, C.; Guo, Y.; He, Z.; Huang, X.; Jia, X.; Yang, T. SARS-CoV-2 and SARS-CoV: Virtual Screening of Potential Inhibitors Targeting RNA-Dependent RNA Polymerase Activity (NSP12). *J. Med. Virol* **2021**, *93*, 389–400, <https://doi.org/10.1002/jmv.26222>.
29. Vyshnava, S.S.; Kanderi, D.K.; Panjala, S.P.; Paramasivam, K.; Pandluru, G.; Banapuram, S.; Anupalli, R.R.; Dowlatabad, M.R. A Computational Approach on the Activity of Hesperidin as Antagonist for Proteins of SARS-CoV-2. *Lett. Appl. NanoBioScience* **2021**, *10*, 2571–2577.
30. UniProt Consortium. UniProt: A Hub for Protein Information. *Nucleic Acids Res* **2015**, *43*, D204–212, <https://doi.org/10.1093/nar/gku989>.
31. Johnson, M.; Zaretskaya, I.; Raytselis, Y.; Merezuk, Y.; McGinnis, S.; Madden, T.L. NCBI BLAST: A Better Web Interface. *Nucleic Acids Res* **2008**, *36*, W5–9, <https://doi.org/10.1093/nar/gkn201>.
32. Biasini, M.; Bienert, S.; Waterhouse, A.; Arnold, K.; Studer, G.; Schmidt, T.; Kiefer, F.; Gallo Cassarino, T.; Bertoni, M.; Bordoli, L.; Schwede, T. SWISS-MODEL: Modelling Protein Tertiary and Quaternary Structure Using Evolutionary Information. *Nucleic Acids Res* **2014**, *42*, W252–8, <https://doi.org/10.1093/nar/gku340>.
33. Laskowski, R.A.; MacArthur, M.W.; Thornton, J.M. PROCHECK: Validation of Protein-Structure Coordinates. In *International Tables for Crystallography*; International Union of Crystallography: Chester, England, **2012**, 684–687, <https://doi.org/10.1107/97809553602060000882>.
34. Yuan, S.; Chan, H.C.S.; Hu, Z. Using PyMOL as a Platform for Computational Drug Design: PyMOL: Platform for Computational Drug Design. *Wiley Interdiscip. Rev. Comput. Mol. Sci* **2017**, *7*, <https://doi.org/10.1002/wcms.1298>.
35. Rahman, A.; Ali, M.T.; Shawan, M.M.A.K.; Sarwar, M.G.; Khan, M.A.K.; Halim, M.A. Halogen-Directed Drug Design for Alzheimer's Disease: A Combined Density Functional and Molecular Docking Study. *Springerplus* **2016**, *5*, <https://doi.org/10.1186/s40064-016-2996-5>.
36. Ekins, S.; Mestres, J.; Testa, B. In Silico Pharmacology for Drug Discovery: Methods for Virtual Ligand Screening and Profiling. *Br. J. Pharmacol* **2007**, *152*, 9–20, <https://doi.org/10.1038/sj.bjp.0707305>.
37. Fukunishi, Y.; Nakamura, H. Prediction of Ligand-Binding Sites of Proteins by Molecular Docking Calculation for a Random Ligand Library: Prediction of Ligand-Binding Sites. *Protein Sci* **2011**, *20*, 95–106, <https://doi.org/10.1002/pro.540>.
38. Kar, S.; Roy, K. How Far Can Virtual Screening Take Us in Drug Discovery? *Expert Opin. Drug Discov* **2013**, *8*, 245–261, <https://doi.org/10.1517/17460441.2013.761204>.
39. Pires, D.E.V.; Blundell, T.L.; Ascher, D.B. PkCSM: Predicting Small-Molecule Pharmacokinetic and Toxicity Properties Using Graph-Based Signatures. *J. Med. Chem* **2015**, *58*, 4066–4072, <https://doi.org/10.1021/acs.jmedchem.5b00104>.
40. Daina, A.; Michielin, O.; Zoete, V. SwissADME: A Free Web Tool to Evaluate Pharmacokinetics, Drug-Likeness and Medicinal Chemistry Friendliness of Small Molecules. *Sci. Rep* **2017**, *7*, <https://doi.org/10.1038/srep42717>.
41. Keiser, M.J.; Roth, B.L.; Armbruster, B.N.; Ernsberger, P.; Irwin, J.J.; Shoichet, B.K. Relating Protein Pharmacology by Ligand Chemistry. *Nat. Biotechnol* **2007**, *25*, 197–206, <https://doi.org/10.1038/nbt1284>.
42. Gfeller, D.; Grosdidier, A.; Wirth, M.; Daina, A.; Michielin, O.; Zoete, V. SwissTargetPrediction: A Web Server for Target Prediction of Bioactive Small Molecules. *Nucleic Acids Res* **2014**, *42*, W32–8, <https://doi.org/10.1093/nar/gku293>.
43. Nejadi Babadaei, M. M.; Hasan, A.; Vahdani, Y.; Haj Bloukh, S.; Sharifi, M.; Kachooei, E.; Haghighat, S.; Falahati, M. Development of Remdesivir Repositioning as a Nucleotide Analog against COVID-19 RNA Dependent RNA Polymerase. *J. Biomol. Struct. Dyn* **2020**, 1–9, <https://doi.org/10.1080/07391102.2020.1767210>.
44. Heald-Sargent, T.; Gallagher, T. Ready, Set, Fuse! The Coronavirus Spike Protein and Acquisition of Fusion Competence. *Viruses* **2012**, *4*, 557–580, <https://dx.doi.org/10.3390/v4040557>.
45. Vincent, M.J.; Bergeron, E.; Benjannet, S.; Erickson, B.R.; Rollin, P.E.; Ksiazek, T.G.; Seidah, N.G.; Nichol, S.T. Chloroquine Is a Potent Inhibitor of SARS Coronavirus Infection and Spread. *Virol. J* **2005**, *2*, <https://doi.org/10.1186/1743-422X-2-69>.
46. Wang, M.; Cao, R.; Zhang, L.; Yang, X.; Liu, J.; Xu, M.; Shi, Z.; Hu, Z.; Zhong, W.; Xiao, G. Remdesivir and Chloroquine Effectively Inhibit the Recently Emerged Novel Coronavirus (2019-NCoV) in Vitro. *Cell Res* **2020**, *30*, 269–271, <https://doi.org/10.1038/s41422-020-0282-0>.
47. Muralidharan, N.; Sakthivel, R.; Velmurugan, D.; Gromiha, M.M. Computational Studies of Drug Repurposing and Synergism of Lopinavir, Oseltamivir and Ritonavir Binding with SARS-CoV-2 Protease against COVID-19. *J. Biomol. Struct. Dyn* **2020**, *39*, 1–6, <https://doi.org/10.1080/07391102.2020.1752802>.
48. Khaerunnisa, S.; Kurniawan, H.; Awaluddin, R.; Suhartati, S.; Soetjipto, S. Potential Inhibitor of COVID-19 Main Protease (Mpro) From Several Medicinal Plant Compounds by Molecular Docking Study. *Preprints* **2020**, <https://doi.org/10.20944/preprints202003.0226.v1>.
49. Midgley, I.; Hood, A.J.; Proctor, P.; Chasseaud, L.F.; Irons, S.R.; Cheng, K.N.; Brindley, C.J.; Bonn, R. Metabolic Fate of ¹⁴C-Camostat Mesylate in Man, Rat and Dog after Intravenous Administration. *Xenobiotica* **1994**, *24*, 79–92, <https://doi.org/10.3109/00498259409043223>.

50. Kitamura, K.; Tomita, K. Proteolytic Activation of the Epithelial Sodium Channel and Therapeutic Application of a Serine Protease Inhibitor for the Treatment of Salt-Sensitive Hypertension. *Clin. Exp. Nephrol.* **2012**, *16*, 44–48, <https://doi.org/10.1007/s10157-011-0506-1>.
51. Göke, B.; Printz, H.; Koop, I.; Rausch, U.; Richter, G.; Arnold, R.; Adler, G. Endogenous CCK Release and Pancreatic Growth in Rats after Feeding a Proteinase Inhibitor (Camostate). *Pancreas* **1986**, *1*, 509–515, <https://doi.org/10.1097/00006676-198611000-00008>.
52. Jia, D.; Taguchi, M.; Otsuki, M. Synthetic Protease Inhibitor Camostat Prevents and Reverses Dyslipidemia, Insulin Secretory Defects, and Histological Abnormalities of the Pancreas in Genetically Obese and Diabetic Rats. *Metabolism* **2005**, *54*, 619–627, <https://doi.org/10.1016/j.metabol.2004.12.005>.
53. Hoffmann, M.; Kleine-Weber, H.; Schroeder, S.; Krüger, N.; Herrler, T.; Erichsen, S.; Schiergens, T.S.; Herrler, G.; Wu, N.-H.; Nitsche, A.; Müller, M.A.; Drosten, C.; Pöhlmann, S. SARS-CoV-2 Cell Entry Depends on ACE2 and TMPRSS2 and Is Blocked by a Clinically Proven Protease Inhibitor. *Cell* **2020**, *181*, 271–280.e8, <https://doi.org/10.1016/j.cell.2020.02.052>.
54. Okamoto, M.; Ono, M.; Baba, M. Potent Inhibition of HIV Type 1 Replication by an Antiinflammatory Alkaloid, Cepharanthine, in Chronically Infected Monocytic Cells. *AIDS Res. Hum. Retroviruses* **1998**, *14*, 1239–1245, <https://doi.org/10.1089/aid.1998.14.1239>.
55. Matsuda, K.; Hattori, S.; Komizu, Y.; Kariya, R.; Ueoka, R.; Okada, S. Cepharanthine Inhibited HIV-1 Cell-Cell Transmission and Cell-Free Infection via Modification of Cell Membrane Fluidity. *Bioorg. Med. Chem. Lett* **2014**, *24*, 2115–2117, <https://doi.org/10.1016/j.bmcl.2014.03.041>.
56. Lipinski, C.A.; Lombardo, F.; Dominy, B.W.; Feeney, P.J. Experimental and Computational Approaches to Estimate Solubility and Permeability in Drug Discovery and Development Settings. *Adv. Drug Deliv. Rev* **2012**, *46*, 4–17, [https://doi.org/10.1016/s0169-409x\(00\)00129-0](https://doi.org/10.1016/s0169-409x(00)00129-0).
57. Ghose, A.K.; Viswanadhan, V.N.; Wendoloski, J.J.A Knowledge-Based Approach in Designing Combinatorial or Medicinal Chemistry Libraries for Drug Discovery. 1. A Qualitative and Quantitative Characterization of Known Drug Databases. *J. Comb. Chem* **1999**, *1*, 55–68, <https://doi.org/10.1021/cc9800071>.
58. Egan, W.J.; Merz, K.M.Jr.; Baldwin, J.J. Prediction of Drug Absorption Using Multivariate Statistics. *J. Med. Chem.* **2000**, *43*, 3867–3877, <https://doi.org/10.1021/jm000292e>.
59. Muegge, I.; Heald, S. L.; Brittelli, D. Simple Selection Criteria for Drug-like Chemical Matter. *J. Med. Chem.* **2001**, *44*, 1841–1846, <https://doi.org/10.1021/jm015507e>.
60. Veber, D.F.; Johnson, S.R.; Cheng, H.-Y.; Smith, B.R.; Ward, K.W.; Kopple, K.D. Molecular Properties That Influence the Oral Bioavailability of Drug Candidates. *J. Med. Chem.* **2002**, *45*, 2615–2623, <https://doi.org/10.1021/jm020017n>.
61. Martin, Y.C. A Bioavailability Score. *J. Med. Chem.* **2005**, *48*, 3164–3170, <https://doi.org/10.1021/jm0492002>.
62. Brenk, R.; Schipani, A.; James, D.; Krasowski, A.; Gilbert, I.H.; Frearson, J.; Wyatt, P.G. Lessons Learnt from Assembling Screening Libraries for Drug Discovery for Neglected Diseases. *ChemMedChem* **2008**, *3*, 435–444, <https://doi.org/10.1002/cmdc.200700139>.
63. Baell, J.B.; Holloway, G.A. New Substructure Filters for Removal of Pan Assay Interference Compounds (PAIS) from Screening Libraries and for Their Exclusion in Bioassays. *J. Med. Chem.* **2010**, *53*, 2719–2740, <https://doi.org/10.1021/jm901137j>.
64. Hann, M.M.; Keserü, G.M. Finding the Sweet Spot: The Role of Nature and Nurture in Medicinal Chemistry. *Nat. Rev. Drug Discov.* **2012**, *11*, 355–365, <https://doi.org/10.1038/nrd3701>.
65. Maideen, N.M.P. Recent Updates in the Pharmacological Management of COVID-19. *Lett Appl NanoBioSci* **2020**, *10*, 1969–1980, <https://doi.org/10.33263/LIANBS101.19691980>.
66. Ertl, P.; Schuffenhauer, A. Estimation of Synthetic Accessibility Score of Drug-like Molecules Based on Molecular Complexity and Fragment Contributions. *J. Cheminform.* **2009**, *1*, <https://doi.org/10.1186/1758-2946-1-8>.